

Azimuthal distributions of fission fragments and α particles emitted in the reactions $^{36}\text{Ar} + ^{238}\text{U}$ at $E/A = 20$ and 35 MeV and $^{14}\text{N} + ^{238}\text{U}$ at $E/A = 50$ MeV

M. B. Tsang, Y. D. Kim, N. Carlin, Z. Chen, C. K. Gelbke, W. G. Gong, W. G. Lynch, T. Murakami,
T. Nayak, R. M. Ronningen, H. M. Xu, and F. Zhu

*National Superconducting Cyclotron Laboratory and Department of Physics and Astronomy,
Michigan State University, East Lansing, Michigan 48824*

L. G. Sobotka, D. W. Stracener, D. G. Sarantites, Z. Majka, and V. Abenante

Department of Chemistry, Washington University, St. Louis, Missouri 63130

(Received 23 February 1990)

Azimuthal correlations between coincident fission fragments and α particles were measured for the reactions $^{36}\text{Ar} + ^{238}\text{U}$ at $E/A = 20$ and 35 MeV and $^{14}\text{N} + ^{238}\text{U}$ at $E/A = 50$ MeV. At all energies, coplanar emission is enhanced. The azimuthal distributions for fission fragments and α particles are decoupled using a simple parametrization. Both azimuthal distributions are highly anisotropic at lower incident energies; these anisotropies decrease with energy. At the highest incident energies, energetic α particles emitted at large transverse momenta appear to be more suited than fission fragments to tag the orientation of the entrance channel reaction plane.

Intermediate energy nucleus-nucleus collisions exhibit a subtle interplay between mean-field and nucleon-nucleon collision dynamics. At low incident energies, the mean field is largely attractive. As a consequence, light particles are predominantly emitted to negative deflection angles in the entrance channel reaction plane.¹⁻⁶ With increasing energy, individual nucleon-nucleon collisions are less hindered by the Pauli exclusion principle and the azimuthal distribution of the emitted particles should become more isotropic. A number of measurements¹⁻⁶ are in qualitative agreement with such expectations. To be more quantitative, however, one must locate the entrance channel reaction plane experimentally and know how accurately it has been determined. Well calibrated techniques for determination of the orientation of the reaction plane are also essential for measurements of triple differential cross sections⁷ $\sigma(E, \theta, \phi)$ and for transverse flow analyses.⁸

In order to explore the distribution of particles in and out of the reaction plane and to explore techniques for reaction plane determination, we have investigated correlations between coincident fission fragments and α particles emitted in the reactions $^{36}\text{Ar} + ^{238}\text{U}$ at $E/A = 20$ and 35 MeV and $^{14}\text{N} + ^{238}\text{U}$ at $E/A = 50$ MeV. The experiment was performed with beams from the K500 cyclotron of Michigan State University. A $^{238}\text{UF}_4$ target of 400 $\mu\text{g}/\text{cm}^2$ areal density was used. Charged particles were detected with 96 plastic CsI(Tl) phoswich detectors of the "Dwarf-Ball-Wall" array developed at Washington University,⁹ which has an angular coverage of about 85% of 4π . Two coincident fission fragments were detected with two X - Y position sensitive multiwire detectors¹⁰ covering angular ranges of $\theta_1 = 36^\circ - 116^\circ$ for $\phi_1 = 0^\circ \pm 10^\circ$ and $\theta_2 = 39^\circ - 89^\circ$ for $\phi_2 = 180^\circ \pm 30^\circ$. Further details of the experimental setup can be found in Refs. 11 and 12. In order to reduce contributions from peripheral collisions, all data were filtered placing the following gates on the fission fragment folding angles $\theta_{\text{ff}} \leq 159^\circ$ and 160° for

$^{36}\text{Ar} + ^{238}\text{U}$ at $E/A = 20$ and 35 MeV, and $\theta_{\text{ff}} \leq 170^\circ$ for $^{14}\text{N} + ^{238}\text{U}$ at $E/A = 50$ MeV. Unless otherwise stated, all angles and energies are given with respect to the laboratory frame of reference. Polar angles with respect to the beam axis are denoted as θ and azimuthal angles are denoted as ϕ .

The left-hand-side panels of Fig. 1 show the azimuthal distributions $Y_\alpha^{\text{ff}}(\phi_\alpha)$ of α particles emitted at $\theta_\alpha = 70^\circ$ and with energy $E_\alpha = 46$ –70 MeV in coincidence with two fission fragments; in our convention, α -particle emission in the fission plane corresponds to either $\phi_\alpha = 0^\circ$ or 180° . (Azimuthal distributions presented in this Rapid Communication are normalized to an average value of unity.) Consistent with previous observations,¹ α particles are preferentially emitted in the fission plane. For the decay of residues with large angular momenta, the fission plane is closely correlated with the entrance channel reaction plane (which is perpendicular to the semiclassical entrance channel orbital angular momentum vector).¹¹ In order to extract the azimuthal anisotropies, $R_\alpha^{\text{ff}} = Y_\alpha^{\text{ff}}(\phi_\alpha = 0^\circ) / Y_\alpha^{\text{ff}}(\phi_\alpha = 90^\circ)$, we have fitted the azimuthal distribution with a simple functional form: $Y_\alpha^{\text{ff}}(\phi_\alpha) \propto \exp(-\kappa \sin^2 \phi_\alpha)$, where κ was treated as an adjustable parameter. Examples of such fits are shown by the dash-dotted curves in the left-hand side panels of Fig. 1. The anisotropies provided by the fits are shown on the right-hand side of Fig. 1, as a function of α -particle kinetic energy $\langle E_\alpha \rangle$ for $\theta_\alpha = 70^\circ$ (top panel), and as a function of emission angle θ_α for $E_\alpha = 46$ –70 MeV (bottom panel). The most pronounced azimuthal asymmetries are observed for high energy α particles emitted at $\theta_\alpha \approx 70^\circ - 90^\circ$. The enhancement of α -particle emission in the fission plane becomes less pronounced with increasing projectile velocity.

Decreasing values of R_α^{ff} correspond to less enhanced emission in the entrance channel reaction plane, for fission fragments, α particles, or both. In order to assess the degree to which emission is enhanced in the entrance chan-

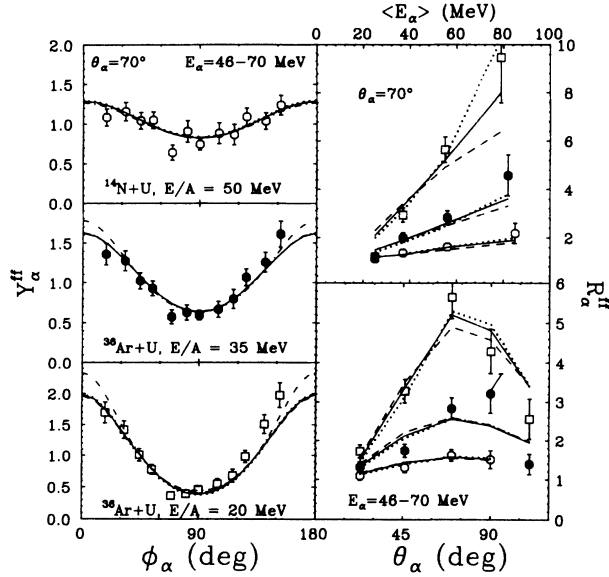


FIG. 1. Left-hand-side panels: Azimuthal distributions Y_{α}^{ff} between fission fragments and α particles for $E_{\alpha}=46-70$ MeV and $\theta_{\alpha}=70^{\circ}$. Right-hand-side panels: In- to out-of-plane ratio R_{α}^{ff} for coincident fission fragments and α particles. The top panel shows the dependence of R_{α}^{ff} on the kinetic energy of α particles emitted at $\theta_{\alpha}=70^{\circ}$; the bottom panel shows the dependence of R_{α}^{ff} on the emission angle for α particles with $E_{\alpha}=46-70$ MeV. Open squares, solid points, and open circles show data for the reactions $^{36}\text{Ar}+^{238}\text{U}$ at $E/A=20$ and 35 MeV and $^{14}\text{N}+^{238}\text{U}$ at $E/A=50$ MeV, respectively. The solid, dashed, dotted, and dash-dotted lines depict calculations described in the text.

nel reaction plane, we assumed that the measured azimuthal correlations result from a convolution of the individual emission patterns of α particles and fission fragments, both of which are enhanced in the entrance channel reaction plane. The two emission patterns were described with respect to the orientation of the entrance channel reaction plane and parametrized as in Refs. 1 and 4. These parametrizations, given below, are chosen because of their simplicity and because they can fit the experimental data rather well. Different functional forms are not expected

to change our qualitative conclusions.

The probability distribution $P(\phi)$ for the angle ϕ between the entrance channel scattering plane and the fission plane was parametrized as¹

$$P_f(\phi) \propto \exp(-C \sin^2 \phi). \quad (1)$$

Semiclassically, $C = \hbar^2 J^2 \sin^2 \theta_f / 2T_f I_{\text{eff}}$, where J , T_f , and I_{eff} are the angular momentum, temperature, and effective moment of inertia, respectively, of the fissioning nucleus, and θ_f is the emission angle (in the rest frame of the fissioning nucleus) of one fragment with respect to the beam direction. For heavy ion induced fission at high angular momenta, the effective moments of inertia are larger than expected from the transition state model.¹³ Moreover, important properties of the fissioning nuclei (recoil velocity, excitation energy, mass, charge, effective moment of inertia, and angular momentum) are not accurately known because of preequilibrium emissions. Thus we treat C as an adjustable parameter.

The emission of α particles was described using an expression for the emission from an ideal gas of temperature T , rotating with angular velocity ω perpendicular to the reaction plane, and moving with a velocity v_0 parallel to the beam axis:^{1,4}

$$P_{\alpha}(E_{\alpha}, \theta_{\alpha}, \phi_{\alpha} - \phi) \propto [(E_{\alpha} - V_c) E_s]^{1/2} \times \frac{J_1(iK)}{iK} \exp(-E_s/T). \quad (2)$$

Here,

$$E_s = E_{\alpha} - V_c + E_0 - 2[E_0(E_{\alpha} - V_c)]^{1/2} \cos \theta_{\alpha},$$

$K = (R\omega/T) \{2m_{\alpha}[E_s - (E_{\alpha} - V_c) \sin^2 \theta_{\alpha} \sin^2(\phi_{\alpha} - \phi)]\}^{1/2}$, and $E_0 = \frac{1}{2} m_{\alpha} v_0^2$; J_1 denotes the first-order Bessel function; E_{α} , m_{α} , θ_{α} , and ϕ_{α} are the energy, mass, polar angle, and azimuthal angle, respectively, of the emitted particle; the parameter V_c corrects for the Coulomb repulsion from the heavy reaction residue, assumed to be at rest in the laboratory.⁴ For comparison to measurements, one must sum over all possible orientations of the reaction plane.¹ Accordingly, the correlations between coincident fission fragments and α particles are given by

$$Y_{\alpha}^{\text{ff}}(E_{\alpha}, \theta_{\alpha}, \phi_{\alpha}) \propto \int_0^{2\pi} d\phi P_f(\phi) P_{\alpha}(E_{\alpha}, \theta_{\alpha}, \phi_{\alpha} - \phi). \quad (3)$$

TABLE I. Parameters used for the calculations shown in Figs. 1 and 2.

Reaction	E/A (MeV)	v_0/c^a	T (MeV) ^b	$R\omega/c$	C	Curve
$^{36}\text{Ar}+^{238}\text{U}$	20	0.08	4.0	0.04	5.2	dotted
				0.05	3.2	solid
				0.06	2.5	dashed
$^{36}\text{Ar}+^{238}\text{U}$	35	0.13	6.0	0.05	3.0	dotted
				0.06	2.2	solid
				0.07	1.8	dashed
$^{14}\text{N}+^{238}\text{U}$	50	0.16	7.5	0.05	1.8	dotted
				0.065	1.2	solid
				0.08	0.9	dashed

^aExtracted from Ref. 17.

^bIn accordance with Ref. 4, this parameter was taken as 0.6 times the slope parameter extracted by a nonrotating moving source analysis of the kinetic-energy spectrum of the emitted particle.

Three calculated correlations between α particles and fission fragments, $Y_{\alpha}^{\text{ff}}(\phi_{\alpha})$, are shown by the solid, dashed, and dotted curves in the left-hand-side panels of Fig. 1. The parameters used for these calculations are listed in Table I. The results of these calculations are nearly indistinguishable. Considerable ambiguities remain concerning the individual α -particle and fission fragment azimuthal distributions because wider fission distributions, $P_f(\phi)$, can be compensated by narrower α -particle distributions, $P_{\alpha}(E_{\alpha}, \theta_{\alpha}, \phi_{\alpha} - \phi)$, without significant effect on the α -fission correlation. In order to reduce these ambiguities, one may explore the azimuthal correlation function for two α particles detected in coincidence with two fission

$$Y_{\alpha\alpha}^{\text{ff}}(\theta_1, \phi_1, \theta_2, \phi_2) \propto \int_0^{2\pi} d\phi \left(P_f(\phi) \int_{\Delta E_1} dE_1 P_{\alpha}(E_1, \theta_1, \phi_1 - \phi) \int_{\Delta E_2} dE_2 P_{\alpha}(E_2, \theta_2, \phi_2 - \phi) \right). \quad (5)$$

An example of such a correlation function for the reaction $^{36}\text{Ar} + ^{238}\text{U}$ at $E/A = 35$ MeV is given in the top panel of Fig. 2. Here, the dependence is shown for the variable $\Delta\phi = \phi_2 - \phi_1$ for fixed angles $\phi_1 = 104^\circ$, $\theta_1 = 42^\circ$, and $\theta_2 = 63^\circ$. The dotted, dashed, and solid curves show calculations performed with the same sets of parameters as for the corresponding curves in Fig. 1. Much of the parameter ambiguity which existed in Fig. 1 for the descrip-

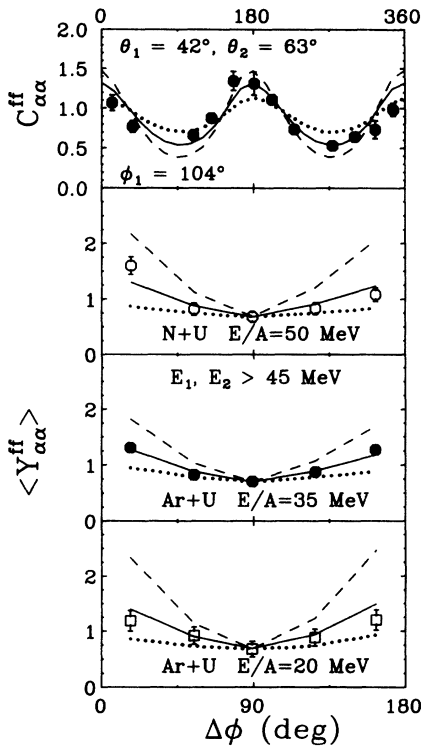


FIG. 2. Top panel: α - α correlation function $C_{\alpha\alpha}^{\text{ff}}$ [Eq. (4)] measured in coincidence with two fission fragments for the $^{36}\text{Ar} + ^{238}\text{U}$ reaction at $E/A = 35$ MeV; the α particles were detected at the polar angles $\theta_1 = 42^\circ$ and $\theta_2 = 63^\circ$ and the azimuthal angles $\phi_1 = 104^\circ$ and $\phi_2 = \phi_1 + \Delta\phi$. Lower panels: Average azimuthal distributions of α particles, $\langle Y_{\alpha\alpha}^{\text{ff}} \rangle$ [Eq. (6)], for the reactions indicated. The solid, dashed, and dotted lines depict calculations described in the text. Energy gates of $E_1, E_2 > 45$ MeV have been applied for all correlations shown.

fragments:

$$C_{\alpha\alpha}^{\text{ff}}(\theta_1, \phi_1, \theta_2, \phi_2) \propto \frac{Y_{\alpha\alpha}^{\text{ff}}(\theta_1, \phi_1, \theta_2, \phi_2)}{Y_{\alpha}^{\text{ff}}(\theta_1, \phi_1) Y_{\alpha}^{\text{ff}}(\theta_2, \phi_2)}. \quad (4)$$

Here, $Y_{\alpha\alpha}^{\text{ff}}(\theta_1, \phi_1, \theta_2, \phi_2)$ denotes the two- α -particle coincidence yield corresponding to the detection of two α particles at the polar and azimuthal angles (θ_1, ϕ_1) and (θ_2, ϕ_2) and two fission fragments at $\phi \approx 0^\circ$ and 180° . In our model parametrization, the single α coincidence yields, $Y_{\alpha}^{\text{ff}}(\theta_1, \phi_1)$ and $Y_{\alpha}^{\text{ff}}(\theta_2, \phi_2)$, are calculated from Eq. (3) after integrating over appropriate energy intervals, ΔE_1 and ΔE_2 . The two- α -coincidence yield is calculated as

tion of $Y_{\alpha}^{\text{ff}}(\phi_{\alpha})$ is now removed in the correlation function $C_{\alpha\alpha}^{\text{ff}}$. Rather than fit a large number of α - α correlation functions measured with moderate statistical accuracy, we have constructed averaged α - α azimuthal distributions, $\langle Y_{\alpha\alpha}^{\text{ff}}(\Delta\phi) \rangle$, defined by

$$\langle Y_{\alpha\alpha}^{\text{ff}}(\Delta\phi) \rangle \propto \sum_{i \neq j} Y_{\alpha\alpha}^{\text{ff}}(\theta_1, \phi_i, \theta_2, \phi_j) \epsilon_{ij}(\Delta\phi) / \sum_{i \neq j} \epsilon_{ij}(\Delta\phi), \quad (6)$$

where $\epsilon_{ij}(\Delta\phi) = 1$ for $\Delta\phi = |\phi_i - \phi_j| \pm 30^\circ$ and $\epsilon_{ij}(\Delta\phi) = 0$ otherwise; the function $\epsilon_{ij}(\Delta\phi)$ selects only those detector pairs for which the difference in azimuthal angles lies within $\Delta\phi \pm 30^\circ$. The summation in Eq. (6) is performed over all detectors i and j which are centered at polar angles $\theta_1 = 40^\circ - 50^\circ$ and $\theta_2 = 60^\circ - 80^\circ$, respectively. Averaged azimuthal α - α distributions obtained from Eq.

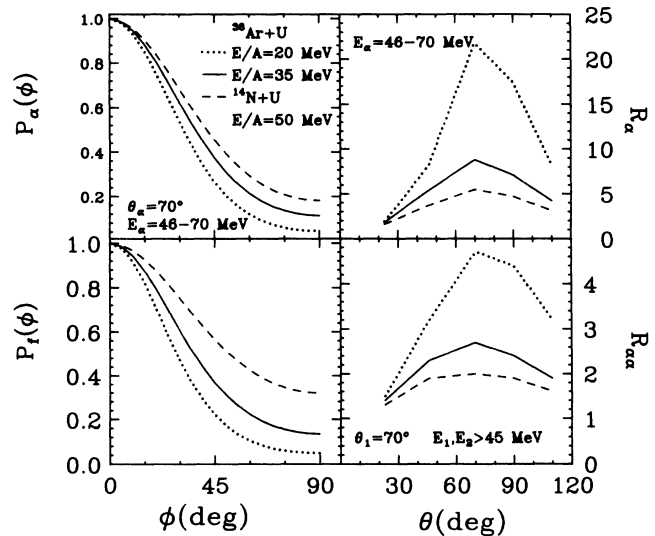


FIG. 3. Left-hand-side panels: Azimuthal distributions, defined with respect to the reaction plane and normalized to unity at $\phi = 0^\circ$, calculated from Eqs. (1) and (2) with the optimum set of parameters for α particles with $E_{\alpha} = 46-70$ MeV and $\theta_{\alpha} = 70^\circ$ (top) and for fission fragments (bottom). Right-hand-side panels: In- to out-of-plane ratio as a function of emission angle for single α -particle distributions with respect to the reaction plane (top) and for azimuthal two- α -correlation functions as a function of the α -particle emission angle θ (bottom).

(6) are shown in the three lower panels of Fig. 2. The dotted, dashed, and solid curves represent calculations, using Eq. (5), for the averaged azimuthal distributions using the same parameter values as in Fig. 1 and taking the individual detector locations into account according to Eq. (6). Most of the parameter ambiguities which existed in the description of the α -fission correlations of Fig. 1 are therefore removed by additional measurements of the average azimuthal α - α distributions. The solid curves in Figs. 1 and 2 represent calculations with an optimum choice of parameters. These calculations also reproduce other overall trends of the data rather well, including the energy and angular dependences shown by the solid lines in the right-hand-side panels of Fig. 1.

Additional insight can be gained by examining the distributions $P_f(\phi)$ and $P_\alpha(E_\alpha, \theta_\alpha, \phi)$, calculated for different orientations of the entrance channel reaction plane, using Eqs. (1) and (2) and the parameters which provide the best description of the experimental data. The α -particle distribution was calculated for $\theta_\alpha = 70^\circ$ using Eq. (2) where the integration is over the α -particle energy range $E_\alpha = 46$ –70 MeV. The left-hand-side panels of Fig. 3 show azimuthal distributions for α particles (top) and fission fragments (bottom) calculated with the optimum parameters for the three reactions. Both fission and α -particle emission become less concentrated in the reaction plane as the projectile energy is increased. Emission out of the reaction plane appears to increase more rapidly for fission than for energetic α particles. The mechanism causing the rapid broadening in the fission distributions is not certain. Broader fission azimuthal distributions could arise from more compact or hotter fission transition states.

$$Y_{\alpha\alpha}(\theta_1, \theta, \Delta\phi) \propto \int_0^{2\pi} d\phi \left[\int_{\Delta E_1} dE_1 P_\alpha(E_1, \theta_1, \phi) \int_{\Delta E_2} dE_2 P_\alpha(E_2, \theta, \phi + \Delta\phi) \right]. \quad (7)$$

Here, P_α is calculated from Eq. (2) and $\Delta E_1 = \Delta E_2 = 46$ –150 MeV; one α particle is detected at $\theta_1 = 70^\circ$ and the other α particle is detected at the polar angle θ . These calculated azimuthal α - α correlations also decrease strongly with projectile velocity, a trend which has been experimentally observed.^{2,4,5,16}

In summary, we have investigated azimuthal correlations between α particles and coincident fission fragments. A simple parametrization has been used to extract the degree to which fission and α -particle emission are enhanced in the entrance channel reaction plane. Both emission patterns become broader as the projectile velocity increases. The most pronounced azimuthal anisotropies are observed for energetic α particles emitted at

Recent measurements of the multiplicities of prefission and postfission neutrons from intermediate energy heavy ion reactions suggest, however, that fission occurs at a rather low temperature during the final stages of these reactions.¹⁴ Therefore, misalignments of the residue angular momentum caused by prefission light particle emission may contribute significantly to the broadening of the fission azimuthal distribution. Energetic α particles, emitted with large transverse momenta during an earlier stage of the reaction, remain strongly aligned in the reaction plane and therefore could be a trigger of choice for tagging the entrance channel reaction plane.

The upper right-hand-side panel in Fig. 3 shows the calculated angular dependence of the ratio

$$R_\alpha = \frac{\int_{\Delta E_\alpha} dE_\alpha P_\alpha(E_\alpha, \theta, 0^\circ)}{\int_{\Delta E_\alpha} dE_\alpha P_\alpha(E_\alpha, \theta, 90^\circ)}$$

of α particles emitted in ($\phi = 0^\circ$) and out ($\phi = 90^\circ$) of the entrance channel reaction plane. Here, P_α is obtained from Eq. (2) and integrated over the interval $46 \text{ MeV} \leq E_\alpha \leq 70 \text{ MeV}$. The largest azimuthal anisotropies are observed for large α -particle emission angles, $\theta \approx 70^\circ$ – 90° . With increasing projectile velocity, the azimuthal distributions become more isotropic. Such an energy dependence is expected from microscopic models which predict enhanced randomization of the particle momenta by nucleon-nucleon collisions at higher incident energies where the Pauli blocking becomes less effective.¹⁵ The lower right-hand-side panel shows the calculated ratio $R_{\alpha\alpha} = Y_{\alpha\alpha}(\Delta\phi = 0^\circ) / Y_{\alpha\alpha}(\Delta\phi = 90^\circ)$, where

$\theta_\alpha \approx 70^\circ$ – 90° ; these particles appear to be better suited than fission fragments to tag the orientation of the entrance channel reaction plane.

The authors wish to acknowledge fruitful discussions with P. Danielewicz and W. Friedman. This work has been supported by the National Science Foundation under Grants No. PHY-86-11210 and No. PHY-89-13813 and by the U.S. Department of Energy under Grants No. DE-FC02-87ER40316 and No. DE-FG02-88ER40406. W.G.L. and L.G.S. acknowledge the receipt of U.S. Presidential Young Investigator Awards. N.C. was partly supported by the Fundação de Amparo e Pesquisa do Estado de São Paulo, Brazil.

¹M. B. Tsang, D. J. Fields, C. K. Gelbke, D. R. Klesch, W. G. Lynch, K. Kwiatkowski, and V. E. Viola, Jr., *Phys. Rev. Lett.* **52**, 1967 (1984).

²P. Kristiansson *et al.*, *Phys. Lett.* **155B**, 31 (1985).

³M. B. Tsang *et al.*, *Phys. Rev. Lett.* **57**, 559 (1986); **60**, 1479 (1988).

⁴M. B. Tsang *et al.*, *Phys. Lett.* **148B**, 265 (1984); C. B. Chitwood *et al.*, *Phys. Rev. C* **34**, 858 (1986).

⁵D. Ardouin *et al.*, *Nucl. Phys.* **A447**, 585c (1985).

⁶D. Fox *et al.*, *Phys. Rev. C* **38**, 146 (1988).

⁷G. M. Welke, M. Prakash, T. T. S. Kuo, and S. Das Gupta, *Phys. Rev. C* **38**, 2101 (1988).

⁸P. Danielewicz and G. Odyniec, *Phys. Lett.* **157B**, 146 (1985).

⁹D. G. Sarantites *et al.*, *Nucl. Instrum. Methods Phys. Res. Sect. A* **264**, 319 (1988); D. W. Stracener *et al.*, *ibid.* (to be published).

- ¹⁰A. Breskin, R. Chechik, Z. Fraenkel, P. Jacobs, I. Tserruya, and N. Zwan, Nucl. Instrum. Methods Phys. Res. Sect. A **221**, 363 (1984).
- ¹¹M. B. Tsang *et al.*, Phys. Lett. B **220**, 492 (1989).
- ¹²Y. D. Kim *et al.*, Phys. Rev. Lett. **63**, 494 (1989).
- ¹³M. B. Tsang, H. Utsunomiya, C. K. Gelbke, W. G. Lynch, B. B. Back, S. Saini, P. A. Baisden, and M. A. McMahan, Phys. Lett. **129B**, 18 (1983); H. Schutte, B. Jäckel, R. A. Esterlund, M. Knaack, W. Westermeier, A. Rox, and P. Patzelt, *ibid.* **232**, 37 (1989).
- ¹⁴D. Hilscher *et al.*, Phys. Rev. Lett. **62**, 1099 (1989).
- ¹⁵M. B. Tsang, G. F. Bertsch, W. G. Lynch, and M. Tohyama, Phys. Rev. C **40**, 1685 (1989).
- ¹⁶W. K. Wilson *et al.*, Michigan State University report (unpublished).
- ¹⁷G. D. Westfall *et al.*, Phys. Lett. **116B**, 118 (1982).